Surface electronic structure and chemisorption on corundum transition-metal oxides: V_2O_3

Richard L. Kurtz* and Victor E. Henrich
Applied Physics, Yale University, New Haven, Connecticut 06520
(Received 23 May 1983)

The surface electronic structure of single-crystal V_2O_3 has been studied by using ultraviolet and x-ray photoelectron spectroscopy. Both nearly-perfect surfaces and surfaces containing point defects have been prepared, and the influence of O_2 and H_2O on both types of surfaces has been investigated. Cation core-level spectra from cleaved surfaces exhibit complex structure. The surface electronic band structure is similar to that of the bulk; at room temperature, V_2O_3 is metallic with the Fermi level E_F lying within the overlapping V($3d$) a_{1g} and e_g^{π} conduction bands. A minimum in the density of states occurs between the V($3d$) and O($2p$) bands at 3 eV below E_F. The O($2p$) valence band has a width of 5.5—6 eV. Surface defects produced by Ar^+-ion bombardment are associated with O vacancies and a net charge transfer to V($3d$) levels. O_2 interacts strongly with both perfect surfaces and surface defects, transferring charge out of the V($3d$) levels and bending both valence and conduction bands up at the surface. The work function rises dramatically, indicating the presence of a negatively charged adsorbed species (likely O^{2-}). H_2O adsorbs dissociatively on both cleaved and bombarded surfaces, producing adsorbed OH^- radicals with a saturation coverage of less than 0.5 monolayer.

I. INTRODUCTION

Transition-metal oxides having the trigonal corundum crystal structure (Ti_2O_3, V_2O_3, Cr_2O_3, and α-Fe_2O_3) comprise a complex and extremely interesting class of materials.[1,2] While their bulk electronic properties have received a good deal of attention in the past, their surface properties are just beginning to be studied. We have initiated a research program exploring the surface electronic and geometric structure of corundum transition-metal oxides, and two previous papers have presented results on the properties of nearly-perfect single-crystal surfaces of Ti_2O_3, the nature of surface defect states, and the chemisorption of O_2 and H_2O on Ti_2O_3.[3,4]

In this paper we report the results of similar measurements on single-crystal samples of vanadium sesquioxide, V_2O_3. Pure V_2O_3 exhibits a strong semiconductor-to-metal transition,[2] and Cr-doped V_2O_3 has complicated conductivity-temperature characteristics that depend strongly upon the Cr doping level.[5] V_2O_3 also exhibits complex paramagnetic and diamagnetic behavior in the bulk.[2] The surface properties of V_2O_3 are particularly interesting since it has the same crystal structure as Ti_2O_3 but one more $3d$ electron on each cation.[1] Comparative studies of Ti_2O_3 and V_2O_3 thus offer the possibility of determining the effects of d-electron population on surface electronic structure and chemisorption activity.

Section II briefly summarizes the bulk structural and electronic properties of V_2O_3, and Sec. III outlines the experimental techniques used in these measurements. Section IV considers the electronic structure of both nearly-perfect, atomically clean V_2O_3 surfaces and the properties of surface defects. The chemisorption of O_2 and H_2O on both nearly-perfect and defect V_2O_3 surfaces is discussed in Secs. V and VI, respectively.

II. BULK PROPERTIES OF V_2O_3

The bulk crystal structure of V_2O_3 is identical to that of Ti_2O_3, with a trigonal primitive cell containing a V_4O_6 basis.[6] The V cations are surrounded by a distorted octahedron of O^{2-} ions and have a $V^{3+}(3d^2)$ electronic configuration. The smallest cation-cation separation is along the threefold trigonal axis, with adjacent cations sharing a

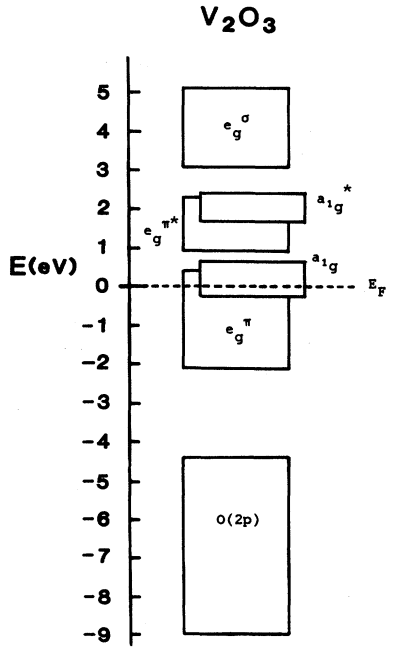

FIG. 1. Empirical band structure of V_2O_3, deduced from previous measurements (see text).

common face of surrounding O octahedra. Above 160 K, V_2O_3 is metallic, with the e_g^{π} and a_{1g} bands overlapping and being partially occupied (see Fig. 1).[2,5] The O($2p$) band has been found from x-ray photoelectron spectroscopy (XPS) measurements to be roughly 6 eV wide[7]; the upper edge of that band has been found from optical measurements to lie about 3.7 eV below the Fermi level E_F.[8] Optical measurements place the bottom of the empty $e_g^{\pi *}$ and a_{1g}^{*} bands at 0.8 and 1.6 eV above E_F, respectively.[9] The doubly degenerate e_g^{σ} band is located about 2.6 eV above E_F. This bulk electronic structure is summarized in the energy-level diagram of Fig. 1.

At about 160 K, V_2O_3 undergoes a first-order transition to a low-temperature semiconducting phase that is accompanied by a trigonal-to-monoclinic structural transformation.[2,5,10] This semiconductor-to-metal transition has been studied by ultraviolet photoemission spectroscopy (UPS) on powder samples, and the difference in the electronic density of states at E_F above and below the transition has been observed.[11,12] Alloying between 0.5 and 1.8 at.% Cr into V_2O_3 produces a new, high-temperature semiconducting phase whose transition temperature depends strongly upon Cr content.[5]

III. EXPERIMENTAL METHODS

The single-crystal V_2O_3 samples used in this work were supplied by Professor J. M. Honig of Purdue University. V_2O_3 cleaves reasonably well along the (047) plane (see Sec. IV), and rods about $4\times4\times25$ mm^3 were oriented by Laue diffraction so that the cleavage plane was perpendicular to the rod axis. Nearly-perfect surfaces were then prepared by cleavage in ultrahigh vacuum (UHV), which resulted in reasonably flat surfaces exhibiting good (1×1) low-energy electron-diffraction (LEED) patterns. The cleaved surfaces were atomically clean as determined by Auger spectroscopy. Defects were produced on cleaved V_2O_3 surfaces by means of 500-eV Ar^+-ion bombardment; the defect density was controlled by varying the bombardment dose. The base pressure of the vacuum system was less than 2×10^{-10} Torr.

UPS spectra were excited with either the He I (21.2-eV) or He II (40.8-eV) lines from a microwave discharge lamp or a hollow cathode dc discharge lamp, respectively. XPS spectra were excited with unmonochromated Al ($K\alpha$) x rays at 1486.7 eV. Photoelectron spectra were obtained with a double-pass cylindrical-mirror spectrometer operating in the retarding mode at a resolution of 240 meV for UPS and 800 meV for XPS spectra. UPS spectra were corrected for the presence of satellite lines in the discharge. Unless noted, no background corrections have been made to the data presented. XPS binding energies are referenced to Au($4f_{7/2}$) at 84.0 eV. The location of E_F was determined from UPS spectra of Au. Auger spectra were excited with an electron gun coaxial with the electron spectrometer, and LEED patterns were displayed on a four-grid 96° LEED optic equipped with a coaxial electron gun.

The O_2 used for chemisorption studies was 99.99% pure. The H_2O used was triply distilled, deionized water contained in a glass vial; details of its purification are given in Ref. 4. An upper limit on the amount of O_2 present in the H_2O is about 500 ppm.[4] Both gases were admitted into the vacuum system through copper-gasket-sealed variable leak valves. The purity of the gases was monitored with a quadrupole mass spectrometer in the UHV chamber.

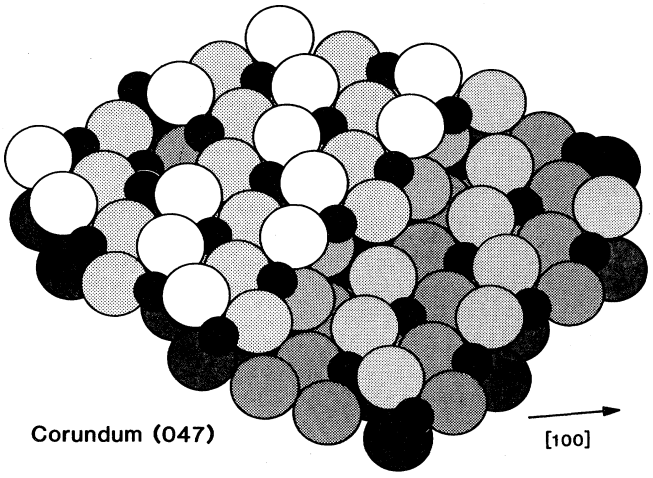

FIG. 2. Model of the corundum (047) surface. Large circles are O anions, small circles are metal cations. Degree of shading indicates depth below the surface. An {047} step to another (047) terrace and an O-vacancy point defect are shown.

IV. SURFACE GEOMETRY AND ELECTRONIC STRUCTURE OF V_2O_3

Single crystals of V_2O_3 were found to cleave preferentially along the same atomic plane as does Ti_2O_3.[3] In rectangular binary-bisectrix-trigonal notation, that plane indexes nearly as (047); in the hexagonal system it indexes exactly as $(10\bar{1}2)$.[13] Figure 2 shows the atomic geometry of that surface; both steps and point defects have been included. Cleavage occurs along the plane of vacant cation sites in the bulk lattice.[13] All cations on the perfect (047) surface are fivefold coordinated by O^{2-} ligands. Cations at step sites are fourfold O coordinated, while point de-

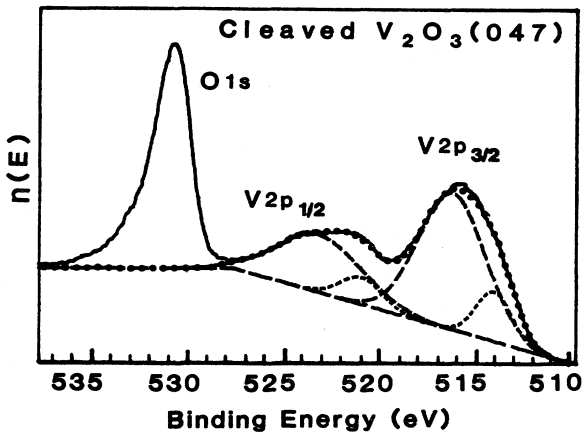

FIG. 3. XPS spectrum for UHV-cleaved V_2O_3(047). See text for details.

fects consisting of O vacancies result in both fourfold- and fivefold-coordinated cations.

A. Nearly-perfect surfaces

Figure 3 shows the XPS spectrum obtained from cleaved $V_2O_3(047)$. The O(1*s*) binding energy is 530.9 eV, and the peak is broadened to the high-binding-energy side, as expected for the scattering mechanisms that dominate in a metallic material.[14,15] The V(2*p*) line shapes are complex, consisting of more than one pair of spin-orbit-split peaks. In order to obtain a qualitative interpretation of the experimental line shapes, we have fitted the XPS spectrum to two pairs of Gaussian functions, after subtraction of a linear background (longest dashed curves in Fig. 2). The two pairs of spin-orbit-split peaks were constrained to have similar relative amplitudes and widths, but the binding energy of the peaks (and hence the magnitude of the spin-orbit splitting) was allowed to vary. The fit shown by the dotted curve yielded binding energies of 516.5 and 523.4 eV for the larger pair of peaks (medium dashed curves) and 514.3 and 521.2 eV for the smaller pair of peaks (short dashed curves). Thus the same spin-orbit splitting, 6.9 eV, was obtained for both pairs of peaks, with the smaller pair shifted to lower binding energy by 2.2 eV.

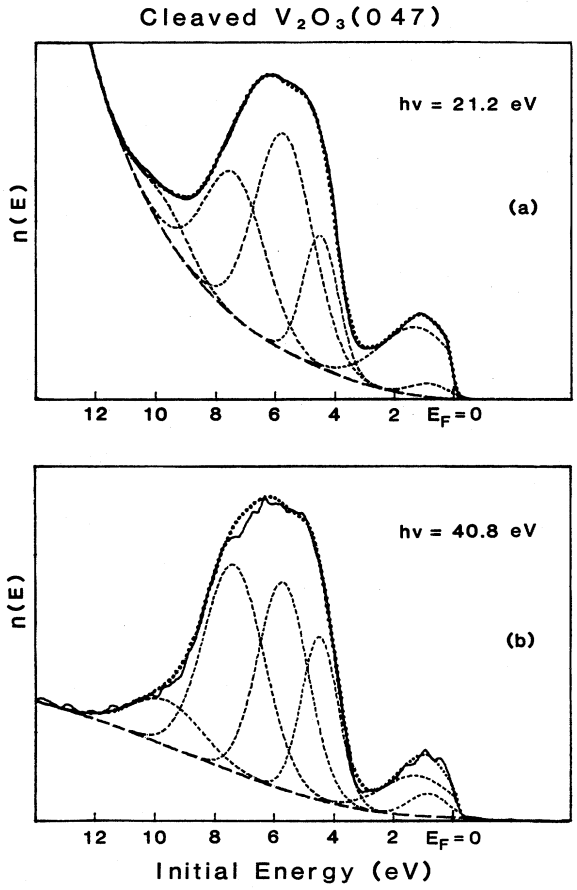

FIG. 4. UPS spectra for UHV-cleaved $V_2O_3(047)$ taken using (a) 21.2-eV and (b) 40.8-eV photons. See text for details.

A detailed analysis of the above XPS results, along with the changes produced by O_2 chemisorption and defect creation, are planned to be published elsewhere.[16] Similar results have been found for nearly-perfect $Ti_2O_3(047)$ surfaces, and, although the origin of the two pairs of peaks is not clear, it is believed to be due to the presence of different discrete-level screening mechanisms for the core holes on the bulk cations.

The He I UPS spectrum for vacuum-cleaved $V_2O_3(047)$ is shown as the solid curve in Fig. 4(a); the solid curve in Fig. 4(b) is the He II spectrum for the same cleaved surface. The large band of emission from 4 to 10 eV below E_F originates from the predominately O(2*p*) valence band, and the emission between E_F and 3 eV arises from the V(3*d*) e_g^π and a_{1g} bands.

In order to obtain a qualitative description of the differences in the measured valence-band spectra for the two photon energies, we have modeled the observed spectra with simple functions. Smooth backgrounds, given by the long dashed curves in Fig. 4, were first subtracted from the spectra (see Ref. 4 for a discussion of background-subtraction techniques). The resultant spectra were then fit with the smallest number of Gaussians that could adequately reproduce the major features of the spectra. Four Gaussians were required for the O(2*p*) band—the same number that was required for Ti_2O_3 (Ref. 4)—and two for the V(3*d*) band; these Gaussians are plotted as short dashed curves in Fig. 4. In both of the spectra the Gaussians have the same energy positions relative to E_F, but their amplitudes and full widths at half maximum (FWHM's) have been independently adjusted to give the best fits. These functions are multiplied by Fermi population and instrumental resolution functions in order to properly reproduce the shape of the spectra in the vicinity of the Fermi level. The locations, widths, and intensities of these Gaussians are given in Table I.

The two peaks that comprise the V(3*d*) band are identified as emission from the e_g^π and a_{1g} bands. This places the center of the e_g^π band about 1.2 eV below E_F and that of the a_{1g} band 0.8 eV below E_F. The total intensity in the V(3*d*) band is smaller for $h\nu$=40.8 eV than for 21.2 eV, paralleling the behavior observed for Ti_2O_3.[4]

The relative intensities of the components of the O(2*p*) valence band also change with photon energy in the same manner for V_2O_3 as they do for Ti_2O_3.[4] It is thus suggestive that for V_2O_3 the cation contribution to the valence

TABLE I. Energy locations (eV), FWHM's (eV), and areas (fraction of total emission intensity) of the Gaussians used in the decomposition of the UPS spectra of fractured $V_2O_3(047)$ plotted in Fig. 4.

		$h\nu$=21.2 eV		$h\nu$=40.8 eV	
Band	Energy	FWHM	Area	FWHM	Area
V(3*d*)	0.84	1.50	0.02	1.50	0.02
	1.24	3.00	0.15	2.70	0.08
O(2*p*)	4.47	1.40	0.14	1.45	0.17
	5.71	2.30	0.38	2.00	0.29
	7.36	2.40	0.26	2.40	0.35
	9.53	1.90	0.05	2.80	0.09

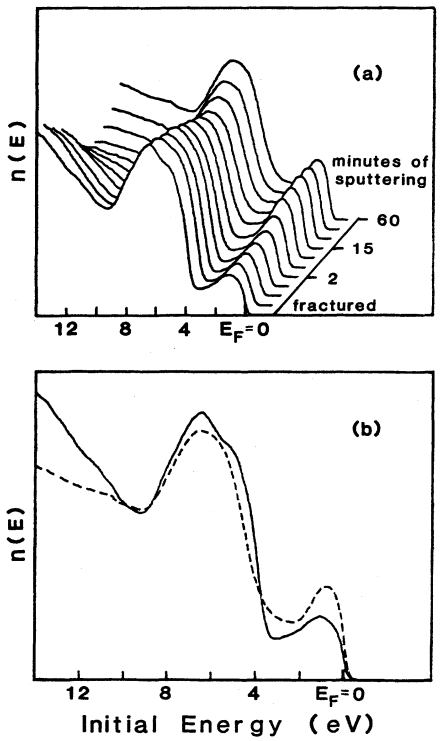

FIG. 5. (a) UPS spectra for Ar^+-ion bombardment of V_2O_3(047) surface for times indicated. (b) UPS spectra for cleaved V_2O_3(047) (solid curve) and equilibrium bombarded surface (dashed curve).

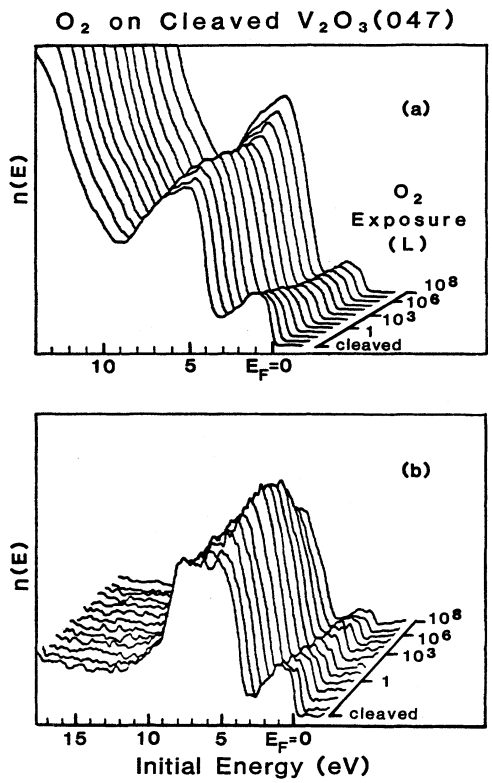

FIG. 6. UPS spectra for exposure of cleaved V_2O_3(047) surface to O_2 taken using (a) 21.2-eV and (b) 40.8-eV photons. (1 L = 1 langmuir = 10^{-6} Torr sec.)

band lies near the lower edge of the band, probably the peak at 7.36 eV below E_F. The increase of the 7.36-eV peak is accompanied by a decrease in V(3d) emission intensity, suggesting different final-state effects for the two photon energies.[4] The O(2p) bandwidth in V_2O_3 is about 1 eV greater than that for Ti_2O_3.

The work function of the cleaved V_2O_3(047) surface, obtained from the cutoff of the inelastic electrons in the 21.2-eV UPS spectrum, was found to be 4.9±0.1 eV, about 1 eV larger than that of Ti_2O_3.[3]

B. Defect V_2O_3 surfaces

The changes in the He I UPS spectrum of V_2O_3 that are produced by Ar^+-ion bombardment of the cleaved surface are illustrated in Fig. 5. A series of UPS spectra for progressively longer bombardment times is shown in Fig. 5(a); Fig. 5(b) compares the spectrum of a cleaved surface with that of the same surface after ion bombardment to its equilibrium state. As with Ti_2O_3, this state is reached after about 15 min of bombardment for the parameters of our ion beam.

Several changes occur in the UPS spectra upon defect formation. The upper edge of the V(3d) band increases in intensity, the band broadens, and defect surface states are introduced into the region of low density of states near 3 eV. The O(2p) band narrows at intermediate defect densities as the upper edge of the band moves away from E_F; the bottom edge of that band remains essentially fixed in energy. The defect surface states near 3 eV appear after about 8 min of sputtering; at that point the O(2p) bandwidth stabilizes to a FWHM that is 0.4 eV less than that of the cleaved surface. The work function decreases by about 0.2 eV after the surface reaches equilibrium defect density.

Auger and XPS data indicate that the surface becomes O deficient under ion bombardment. This is mirrored in an increase in the V(3d) emission intensity and a decrease in the O(2p) intensity in the UPS spectra. From the magnitude of those changes we can estimate the spatial extent of the region that is damaged by ion bombardment. If we assume that the average composition of the damaged surface region has a V:O ratio of 1, that the V ions in this region have a $3d^3$ electronic configuration (versus $3d^2$ in V_2O_3), and that the electron mean free path is 5 Å for emission from the V(3d) band and 8 Å for the O(2p) band, we find that a surface region 3.1 Å thick would produce relative UPS emission intensities similar to those observed.

V. CHEMISORPTION OF O_2 on V_2O_3

When vacuum-fractured V_2O_3(047) is exposed to O_2, the UPS spectra shown in Fig. 6 are obtained. Figures 6(a) and 6(b) show the He I and He II spectra, respectively, for O_2 exposures up to 10^8 langmuir (1 L = 10^{-6} Torr sec); both sets of spectra were taken at the same time from the same cleaved surface. A puzzling effect was observed for

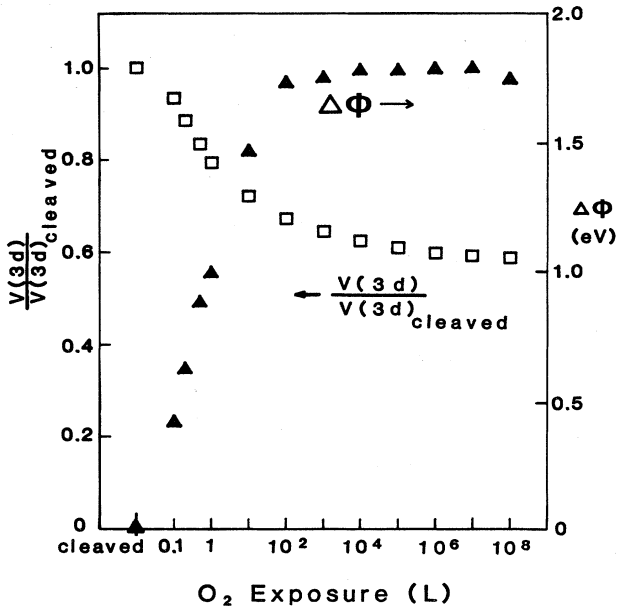

FIG. 7. Changes in work function, $\Delta\phi$, and d-band emission intensity for cleaved $V_2O_3(047)$ exposed to O_2.

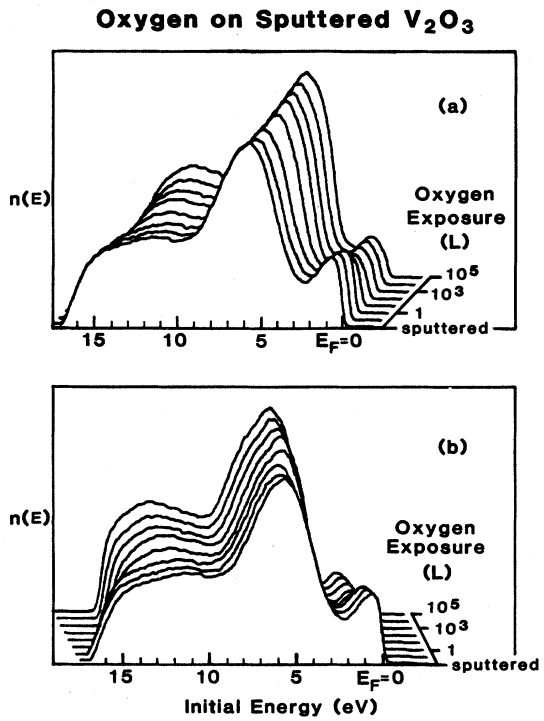

FIG. 8. UPS spectra for ion-bombarded V_2O_3 exposed to O_2. The same data are presented in (a) and (b).

exposures of 10^4 L and up: The intensity of the entire spectrum increased smoothly with exposure. A similar effect was observed for O_2 exposure of α-$Fe_2O_3(001)$ surfaces.[17] The increase does not correlate with changes in any band-structure parameters or with the work function. We have been unable, however, to determine any instrumental cause for the effect. This increase has been removed from the spectra in Fig. 6 by scaling the spectra for 10^4—10^8 L so that the d-band intensity drops smoothly with exposure. No major changes in the spectra occur above 10^3 L, so this normalization is of little significance. However, absolute amplitudes cannot be determined above 10^3 L.

The most striking effect of the chemisorption of O_2 on V_2O_3 is the increase in the work function ϕ by nearly 1.8 eV, which is shown in Fig. 7. This increase correlates with a transfer of electrons out of the V($3d$) band, indicating the creation of negative adsorbed species. The rate of change of ϕ indicates an initial sticking coefficient of 0.01—0.1; completion of the first adsorbed layer seems to inhibit additional adsorption.

The surface band structure also exhibits marked changes upon O_2 chemisorption. In addition to decreasing in intensity (Fig. 7), the bottom of the V($3d$) band moves toward E_F with O_2 exposure, stabilizing by 100 L to a value 0.2 eV above that for the cleaved surface. Even after the highest O_2 exposures, the V($3d$) emission exhibits a significant density of states at the Fermi level. The O($2p$) band exhibits qualitatively different changes than those of the V($3d$) band. Over the range of O_2 exposures investigated, its upper edge moves toward E_F logarithmically; by 10^8 L it has moved 0.4 eV, and its width has decreased by 0.5 eV. Owing to the large changes in surface band structure upon O_2 adsorption, it is not possible to take UPS difference spectra. The narrowing of both the O($2p$) and the V($3d$) bands introduces spurious structure into the differences, regardless of band alignment.

When a high-defect-density V_2O_3 surface is exposed to O_2, the UPS spectra shown in Fig. 8 are obtained; Figs. 8(a) and 8(b) display the same data viewed from different angles. The intensity of emission from the V($3d$) band decreases with O_2 exposure, accompanied by an increase in the emission from the O($2p$) band; by 10^5 L the ratio of the area under the V($3d$) band to that under the O($2p$) band has decreased by 50%. The density of states at the Fermi level drops by a factor of 3, and the V($3d$) and O($2p$) band shapes approach those of cleaved V_2O_3. The O($2p$) valence band moves toward E_F with increasing exposure, rising 0.5 eV by 10^5 L; its width is roughly constant throughout the range of exposures. The work function ϕ increases by 1.5 eV by an O_2 exposure of 100 L, indicating the presence of negative adsorbed species.

VI. CHEMISORPTION OF H_2O on V_2O_3

When a cleaved $V_2O_3(047)$ surface is exposed to successively larger amounts of H_2O, the He I UPS spectra shown in Fig. 9(a) are obtained. Emission from the upper edge of the V($3d$) band decreases during the first 0.2-L exposure, indicating that electrons are transferred out of the a_{1g} band (see Fig. 1). A broad feature appears in the region of the O($2p$) valence band between 4 and 8 eV, and a peak appears at about 10 eV. The O($2p$) band does not exhibit dramatic changes in width, and the bands do not bend significantly. For H_2O exposures below 10 L, the upper edge of the O($2p$) band moves away from E_F by about 0.15 eV; for exposures above 10 L it rises again, but only to a position 0.2 eV above its location for the cleaved surface. The

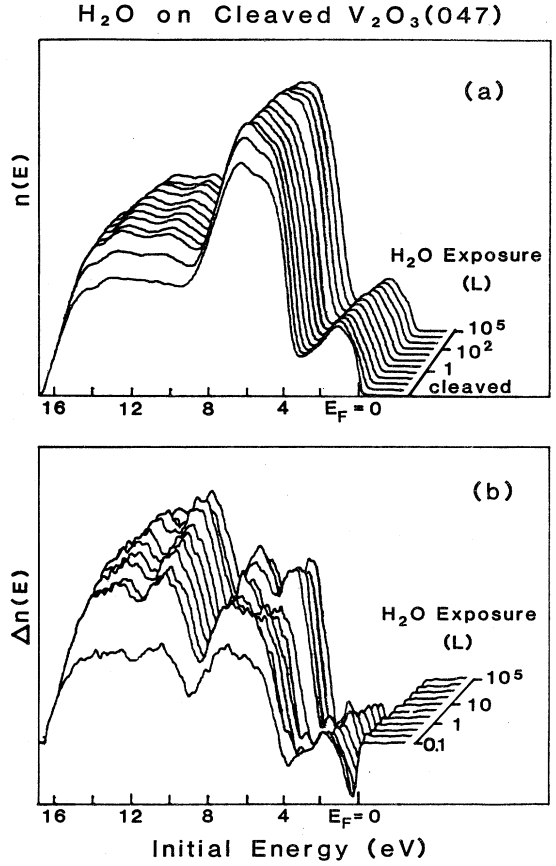

FIG. 9. (a) UPS spectra for cleaved $V_2O_3(047)$ exposed to H_2O. $h\nu=21.2$ eV. (b) Difference spectra for data in (a).

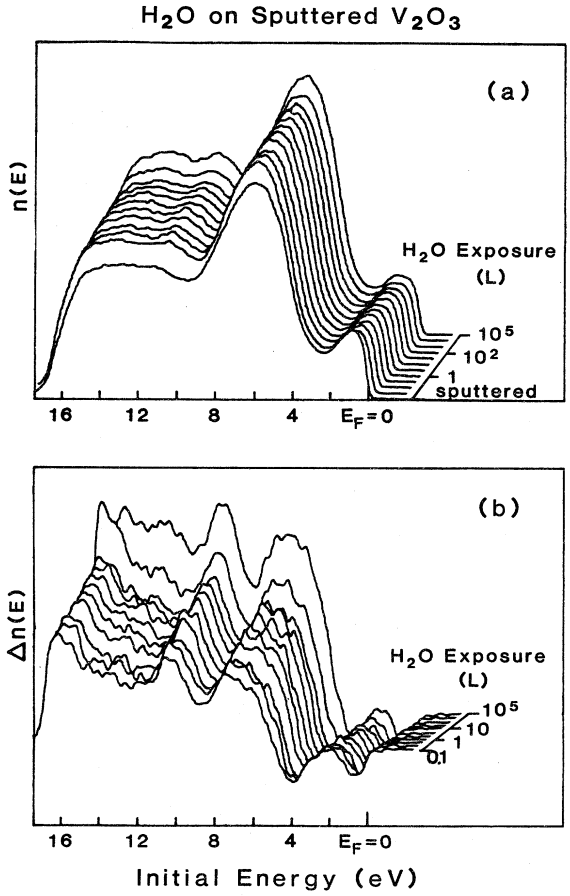

FIG. 10. (a) UPS spectra for ion-bombarded V_2O_3 exposed to H_2O. $h\nu=21.2$ eV. (b) Difference spectra for data in (a).

bottom of the V($3d$) band rises by 0.3 eV. The work function decreases at low exposures, dropping by 0.13 eV by 2 L. Above 10 L, ϕ rises slightly.

There are very few changes in the UPS spectra for H_2O on $V_2O_3(047)$ for exposures above 10^3 L, so O_2 contamination of the H_2O does not appear to be a problem. The slight increase in ϕ at high exposures could be due to O_2 chemisorption, however, since even small O_2 exposures increase ϕ dramatically (see Fig. 7).

Owing to the relative stability of the O($2p$) valence band, it is possible to produce difference spectra from these data. Since the new features that appear in the UPS spectra overlap or lie below the O($2p$) valence band, we have aligned the upper edge of that band before taking differences; the resulting difference spectra are shown in Fig. 9(b). The rapid depopulation of the upper edge of the V($3d$) band appears as a negative peak just below E_F. Two large features appear at 7.4 and 10.7 eV, their amplitudes saturating by 0.2 L; there may also be a third peak at about 14 eV below E_F. Above 10^2 L the O($2p$) valence band broadens, producing a peak in the difference spectra at about 5 eV below E_F.

As discussed in Sec. IV, the creation of defects on a cleaved V_2O_3 surface reduces the surface O concentration, producing a more metallic surface region. When such a high-defect-density surface is exposed to H_2O, the UPS spectra displayed in Fig. 10(a) are obtained. Chemisorption is rapid, and several changes in the spectra occur by 0.2-L exposure. The amplitude of the V($3d$) band emission decreases slightly, while the bottom edge of the O($2p$) band exhibits an increase in amplitude; a new peak also appears at about 10.5 eV below E_F. The work function drops rapidly with increasing exposure, falling by 0.25 eV by 1 L.

Since the O($2p$) valence band for the sputtered V_2O_3 surface is perturbed by H_2O exposure even less than that of the fractured surface, difference spectra can be produced without any shifting of the spectra; the resulting differences are displayed in Fig. 10(b). In addition to the depopulation of the V($3d$) band, two features arise, centered at 6.9 and 10.2 eV, and there is a strong depopulation of the defect surface states located between the O($2p$) and V($3d$) bands. Adsorption is essentially complete by 0.2 L. Again, there is no evidence for O_2 chemisorption at high H_2O exposures.

VII. DISCUSSION

The fact that both V_2O_3 and Ti_2O_3 cleave along the same (047) crystal plane makes them excellent materials on which to study the effects of surface cation d-electron

population on surface electronic structure and chemisorption.[1] It must be borne in mind that the quality of cleaved $V_2O_3(047)$ surfaces is inferior to that of $Ti_2O_3(047)$, so V_2O_3 will possess a higher density of surface steps. In most cases, however, the effects of these steps appear to be small.

The shapes of the O($2p$) valence bands for V_2O_3 and Ti_2O_3 are very similar, as can be seen by comparing the Gaussian fits to that band for the two materials.[4] Four Gaussians are required in both cases, and their relative positions in energy are the same to within 0.25 eV for both materials. There are differences in the relative amplitudes of the peaks, but in both cases the third peak from the top of the band increases in amplitude more upon going from 21.2- to 40.8-eV photons than do the other peaks. Since the admixture of cation wave functions to the primarily O($2p$) valence band is expected to lie in the lower half of that band [i.e., the region of the bonding O($2p$) orbitals],[1] the third peak might represent the cation contribution; similar considerations apply to Ti_2O_3.[3,4] This is only a qualitative interpretation, however, since our deconvolution procedure has no theoretical basis other than to reproduce the observed band shapes. In order to uniquely identify the cation contribution it would be necessary to compare the measured spectra with a photoemission density of states based on a theoretical calculation, such as has been done for $SrTiO_3$.[18]

The metallic nature of the cleaved V_2O_3 surface is evident from the magnitude of the electron emission at E_F (Fig. 4); this is in contrast to semiconducting Ti_2O_3, where cleaved surfaces exhibited much smaller emission at E_F.[3,4] The density of occupied states at E_F becomes even larger when defects are created on V_2O_3 (Fig. 5), which is consistent with the reduction of the surface and the probable formation of $V^{2+}(3d^3)$ ions or perhaps even some metallic V^0. (These effects have been seen in XPS spectra of ion-bombarded Ti_2O_3 surfaces.[17]) The changes in the V($3d$) and O($2p$) bands upon defect creation also parallel those seen for Ti_2O_3.[3]

It is interesting to note the absence of a formal band gap between the cation and anion bands in V_2O_3; a 2.5-eV gap was observed for Ti_2O_3.[3,4] The overlap of the O($2p$) and V($3d$) bands is not predicted by Goodenough's semiempirical band-structure model,[2] and it apparently is not a feature of more detailed calculations.[19] Since none of the surface treatments investigated significantly altered this band overlap, it is unlikely that the states in this region are surface states. This overlap does agree with previous XPS measurements[7] but has yet to be explained theoretically.

The interaction of O_2 with cleaved $V_2O_3(047)$ is qualitatively similar to that for Ti_2O_3,[3] but there are large quantitative differences. The work-function increase when either cleaved or defect V_2O_3 surfaces are exposed to O_2 is 3—4 times larger than that for Ti_2O_3. The accompanying decrease in the intensity of emission from the cation band is smaller for V_2O_3, however. Although difference spectra cannot be taken for O_2 exposure due to complex changes in band structure, the adsorbed species is clearly negative, most likely O^{2-} ions completing the octahedral O coordination of the surface cations.

Interpretation of the adsorption of H_2O on Ti_2O_3 was not without ambiguities[4]; such is the case for V_2O_3 also. The UPS spectra for H_2O on cleaved $V_2O_3(047)$, Fig. 9, clearly show that the adsorbed species interacts strongly with the a_{1g} part of the V($3d$) band, since even 0.1-L exposure depopulates the upper edge of the band. There is very little interaction with the lower part of the band, where the dominant contribution is from the e_g^{π} orbitals. The a_{1g} orbital ($d_{3z^2-r^2}$) points along the trigonal axis, so on the (047) surface its lobe of charge is inclined 32° up from the macroscopic surface plane. The e_g^{π} orbitals, on the other hand, point more nearly normal to the surface in the direction of the missing cation ligand in the basal plane.

Although no unambiguous fingerprint of either adsorbed OH^- or H_2O is apparent in the difference spectra of Fig. 9(b), the spectra are dominated at low exposures by a two-peaked structure. A third, weak peak at about 14 eV is also present for all but the lowest exposures; however, it lies very close to the vacuum cutoff in the He I spectra. He II spectra for H_2O on cleaved $V_2O_3(047)$ exhibit the same two strong peaks seen in Fig. 9(b), but there is no compelling evidence for a peak at 14 eV. We thus conclude that dissociative adsorption of OH^- predominates on this surface. We identify the peaks at 7.4 and 10.7 eV as the 1π and 3σ molecular orbitals of OH^-, respectively.[20,21] The observed peak separation, 3.3 eV, is in excellent agreement with observations of OH^- adsorbed on Pt; the extramolecular relaxation-polarization (ERPS) shifts are also nearly the same.[21] Since adsorption depopulates the a_{1g} band preferentially, it is probable that chemisorption consists of σ bonding between the substrate cation a_{1g} and O lone-pair orbitals of OH^-. The dipole moment of OH^- would be in a direction such as to lower the work function, but its orientation would result in a relatively small decrease in ϕ, as observed at low exposures. We cannot rule out the possibility of some molecular adsorption of H_2O on this surface due to the (possible) presence of the weak peak at 14 eV. The dipole moment of H_2O would also tend to decrease ϕ.

Since the step density on cleaved $V_2O_3(047)$ is relatively large, as determined from the quality of the LEED patterns, it is possible that OH^- adsorption occurs preferentially at step sites. The above arguments concerning molecular orientation would apply to both terraces and steps, however.

The interaction of H_2O with high-defect-density V_2O_3 surfaces, Fig. 10, is easier to interpret. The two-peaked difference spectra of Fig. 10(b) indicate that H_2O absorbs dissociatively on high-defect-density V_2O_3 surfaces. Charge is transferred out of the defect surface states and the V($3d$) band, producing adsorbed OH^- radicals. The 1π-3σ peak separation is identical to that observed for OH^- on fractured V_2O_3, and although the peak locations relative to E_F are the same, OH^- on the more metallic sputtered surface experiences an ERPS shift that is greater by 1 eV. The decrease in work function implies the presence of a net dipole moment directed away from the surface. This is consistent with the chemisorption of OH^- radicals via their O atoms, increasing the ligand coordination of surface V cations.

VIII. SUMMARY

We have studied nearly-perfect and defect $V_2O_3(047)$ surfaces, measuring their electronic structures and investigating the nature of their interactions with O_2 and with H_2O. Vacuum-fractured V_2O_3 exhibits a complex V($2p$) core-level line shape, which is believed to arise from discrete-level final-state screening of core holes. This effect has previously been observed in Ti_2O_3 but is absent in α-Fe_2O_3, where the cation d bands lie further below the Fermi level. The surface band structure of V_2O_3 is similar to that of the bulk, with the partially populated V($3d$) a_{1g} and e_g^{π} conduction bands slightly overlapping the 5.5—6 eV wide O($2p$) valence band. Point defects induced by Ar^+-ion bombardment result in an O-deficient surface with an attendant charge transfer to surface V cations, producing defect surface states between the V($3d$) and O($2p$) bands. Exposure of the fractured surface to O_2 increases the work function dramatically, indicating the presence of negatively charged adsorbed species, probably O^{2-}. Charge transfer from the d band to adsorbed species is evident in the UPS spectra. The defect surface exhibits similar changes upon O_2 chemisorption. When either cleaved or ion-bombardment V_2O_3 surfaces are exposed to H_2O, the work function decreases and the UPS difference spectra exhibit a double-peaked structure characteristic of adsorbed OH^-. This is in contrast to the case of H_2O chemisorption on Ti_2O_3, where the cleaved (047) surface was found to chemisorb water molecularly while dissociative chemisorption occurred on the defect surface. On both the cleaved and bombarded $V_2O_3(047)$ surfaces, saturation coverage is reached at exposures of less than 0.5 L, paralleling the behavior exhibited by Ti_2O_3.

The surface properties of V_2O_3 and Ti_2O_3, which differ primarily in the presence of an additional $3d$ electron on the $V^{3+}(3d^2)$ cations, are thus qualitatively similar, although quantitative differences exist. The only major difference appears to be the dissociative chemisorption of H_2O on cleaved V_2O_3 surfaces. This could arise from the different electronic configurations, but the existence of a greater density of steps on V_2O_3 allows the possibility of preferential adsorption at step sites.

ACKNOWLEDGMENTS

The authors are grateful to Professor J. M. Honig of Purdue University for supplying the V_2O_3 samples and J. M. McKay and H. R. Sadeghi for valuable discussions. This work was partially supported by the National Science Foundation under Grants Nos. DMR-78-23963 and DMR-82-02727.

---

*Present address: Surface Science Division, National Bureau of Standards, Washington, D.C. 20234.

[1]V. E. Henrich, Prog. Surf. Sci. 14, 175 (1983).
[2]J. B. Goodenough, in *Progress in Solid State Chemistry,* edited by H. Reiss (Pergamon, New York, 1972).
[3]R. L. Kurtz and V. E. Henrich, Phys. Rev. B 25, 3563 (1982).
[4]R. L. Kurtz and V. E. Henrich, Phys. Rev. B 26, 6682 (1982).
[5]H. Kuwamoto, J. M. Honig, and J. Appel, Phys. Rev. B 22, 2626 (1980).
[6]R. W. G. Wyckoff, *Crystal Structures* (Interscience, New York, 1964), Vol. 2.
[7]G. A. Sawatzky and D. Post, Phys. Rev. B 20, 1546 (1979).
[8]P. Shuker and Y. Yocoby, Phys. Rev. B 14, 2211 (1976).
[9]I. Balberg, Phys. Lett. 43A, 497 (1973).
[10]H. J. Zeiger, Phys. Rev. B 11, 5132 (1975).
[11]N. Beatham, I. L. Fragala, A. F. Orchard, and G. A. Sawatzky, J. Chem. Soc. Faraday Trans. II 76, 929 (1980).
[12]N. Beatham, A. F. Orchard, and G. Thornton, J. Phys. Chem. Solids 42, 1051 (1981).
[13]I. P. Kaminow, E. H. Turner, R. L. Barns, and J. L. Bernstein, J. Appl. Phys. 51, 4379 (1980).
[14]S. Doniach and M. Šunjić, J. Phys. C 3, 285 (1970).
[15]G. K. Wertheim and S. Hüffner, Phys. Rev. Lett. 35, 53 (1975).
[16]R. L. Kurtz, J. M. McKay, and V. E. Henrich (unpublished).
[17]R. L. Kurtz, Ph.D. thesis, Yale University, 1983 (unpublished).
[18]S. Ellialtioğlu, T. Wolfram, and V. E. Henrich, Solid State Commun. 27, 321 (1978).
[19]J. Ashkenazi and T. Chuchem, Philos. Mag. 32, 763 (1975).
[20]J. A. Connor, M. Considine, I. H. Hillier, and D. Briggs, J. Electron Spectrosc. Relat. Phenom. 12, 143 (1977).
[21]G. B. Fisher and B. A. Sexton, Phys. Rev. Lett. 44, 683 (1980).